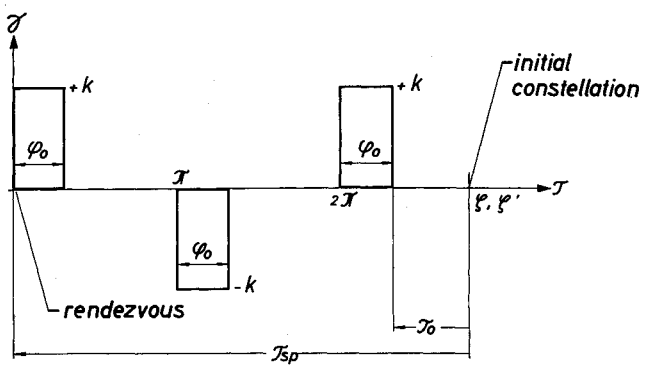

Fig. 2 Control program, spatial component.

Hohmann phase. Now one obtains

$$\varphi_3 = \varphi_2(\delta + \varphi_2/2)/(n\pi - \varphi_2)$$
$$\tau_1 = 0 \qquad \tau_2 = n\pi + \varphi_3 \tag{19}$$

The other data remain unchanged again. The velocity requirement number is greater than the optimum value and increases, for fixed n, with increasing phase difference between S and T. The difference between C_{p1} and ξ_1, however, may be adequately compensated by choice of suitable duration of the maneuver. We have achieved the optimum in the sense of Pontrjagin. The Pontrjagin switching function for the limit case $k \to \infty$ (impulses) is given in closed form by

$$\chi(\tau) = -1 + (1 - \cos\tau)/2n + (\tau + \sin\tau)/n\pi \tag{20}$$

Equation (2) describing the spatial component of motion also admits a simple closed solution. In Fig. 2 the control is demonstrated. We provide firing intervals all of a fixed duration φ_0, with maximum magnitude of acceleration and alternating sign. These intervals are separated by coasting periods of duration $\pi - \varphi_0$. At the beginning a proper coasting time τ_0 is located. It is easily confirmed by (2) that

$$tg(\tau_0 + \varphi_0/2) = \xi/\xi' \qquad \sin(\varphi_0/2) = (\zeta^2 + \zeta'^2)^{1/2}/2km \tag{21}$$

holds; m has to be chosen large enough, so that φ_0 can be determined by (21). The resulting velocity requirement number is given by

$$C_{sp} = km\varphi_0 = (\zeta^2 + \zeta'^2)^{1/2}(\varphi_0/2)/\sin(\varphi_0/2) \tag{22}$$

This formula shows that C_{sp} tends to the absolute optimum $(\zeta^2 + \zeta'^2)^{1/2}$, if m tends to infinity. We have achieved the optimum in the sense of Pontrjagin. The corresponding switching function is as follows:

$$\chi(\tau) = \cos(\tau - \varphi_0/2)/\cos(\varphi_0/2) \tag{23}$$

Concluding Remarks

The following statements must be taken into account for a low-fuel rendezvous maneuver: 1) the initial orbit of the space vehicle should lie within the target orbit; 2) there should be an angular difference between the two bodies such that the space vehicle lags behind the Hohmann phase; and 3) deviations from 2) can be compensated by a sufficient maneuver time. Numerical solutions to most optimization problems can be obtained by the well-known methods of the calculus of variations, but they rarely provide theoretical insight. They are indispensable, of course, but science is asked to find general properties as the backbone of computer solutions. This note has answered such questions for the case of rendezvous to a circular moving target.

References

[1] Clohessy, W. R. and Wiltshire, R. S., "Terminal guidance system for satellite rendez-vous," J. Aerospace Sci. **27**, 653 (1960).

[2] Pontrjagin, L. S., Boltjanskij, V. G., Gamkrelidze, R. V., and Miscenko, E. F., *Mathematische theorie optimaler prozesse* (R. Oldenbourg, Munich, Germany, 1964); translation from Russian, 1960.

[3] Goldstein, A. A. and Seidman, T. I., "Fuel optimization in orbital rendez-vous," Math. Note 317, Mathematics Research Lab., Boeing Scientific Research Labs., DI-82-0292 (August 1963).

[4] Goldstein, A. A., Greene, A. H., Johnson, A. T., and Seidman, T. I., "Fuel optimization in orbital rendez-vous," *AIAA Progress in Astronautics and Aeronautics: Guidance and Control—11*, edited by R. C. Langford and C. T. Mundo (Academic Press, New York, 1964), Vol. 13, pp. 823–844; also AIAA Preprint 63-354 (August 1963).

[5] Tschauner, J. and Hempel, P., "Optimale Beschleunigungsprogramme für das Rendezvous-Manöver," Astronaut. Acta **X**, 296–307 (1964).

[6] Kalman, R. E., Ho, Y. C., and Narendra, K. S., "Controllability of linear dynamical systems," Contrib. to Differential Equations, I, 189–213 (1962).

[7] Hempel, P. und Tschauner, J., "Uber Beschleunigungsprogramme minimaler Übergangsenergie für das Rendezvous-Manöver," Astronaut. Acta **X**, 221–237 (1964).

Stresses in an Ablating, Viscoelastic, Case-Bonded Cylinder

A. J. Mikeska*
Atlantic Research Corporation, Alexandria, Va.

SIGNIFICANT strains during pressurization of a ported propellant grain will usually occur near star points (or near the inside radius of a smooth bore grain). Viscoelastic behavior of the propellant and elastic behavior of the motor case will control the magnitude of these strains. Pressurization rate and burning rate will dictate the rise of strain at a particular location and the time at which that location disappears. As a first step toward calculating grain behavior for a realistic burning history, it was decided to confine the analysis to an idealized geometry, e.g., a case-bonded cylinder under plane strain or plane stress. As indicated later, an elastic solution, which takes into account the actual end conditions (and appropriate stress concentration factors), should provide a sufficiently accurate correction to the solution for the ideal geometry. Thus, it was postulated that the important quality of the analysis was to be the retention of realistic conditions of pressurization and ablation. In this light, other simplifications, such as linear viscoelastic behavior, small deformations, and propellant incompressibility and isotropy are assumed.

Formulation

For an orthogonal, curvilinear coordinate system, propellant response is formulated by the Boltzmann superposition integral

$$e_{ij} = \frac{1}{2}\int_0^{t_n} \Phi(t_n - t)\,\frac{\partial}{\partial t}\,S_{ij}dt \tag{1}$$

where e_{ij} and S_{ij} are the deviatoric components of the strain and stress tensors, and $\Phi(t)$ is a creep compliance function for shear

$$e_{ij} = \epsilon_{ij} - \tfrac{1}{3}\delta_{ij}\theta \qquad S_{ij} = \sigma_{ij} - \tfrac{1}{3}\delta_{ij}\Theta$$

Presented as Preprint 65-177 at the AIAA 6th Solid Propellant Rocket Conference, Washington, D. C., February 1–3, 1965; revision received April 7, 1965.

* Analytical Engineer.

where

$$\theta = \epsilon_{11} + \epsilon_{22} + \epsilon_{33} \qquad \Theta = \sigma_{11} + \sigma_{22} + \sigma_{33}$$

For an incompressible material, $\theta = 0$. Furthermore, the quantity readily available from uniaxial testing is not $\Phi(t)$, but the uniaxial creep compliance $D(t) \equiv \frac{1}{3}\Phi(t)$. Making these substitutions, Eq. (1) becomes

$$\epsilon_{ij} = \frac{3}{2}\int_0^{t_n} D(t_n - t)\frac{\partial}{\partial t}\left[\sigma_{ij} - \frac{1}{3}\delta_{ij}\Theta\right]dt \qquad (2)$$

For the ideal geometries there is no shear stress in the coordinate directions, leaving the three normal components of strain

$$\epsilon_{11} = \int_0^{t_n} D(t_n - t)\frac{\partial}{\partial t}\left[\sigma_{11} - \frac{1}{2}(\sigma_{22} + \sigma_{33})\right]dt \qquad (3)$$

and ϵ_{22} and ϵ_{33}, for which the last parenthetic term becomes $(\sigma_{11} + \sigma_{33})$ and $(\sigma_{11} + \sigma_{22})$, respectively. Also, the propellant stress problem can be considered as a first boundary-value problem involving internal pressure (P_0), case-to-propellant interface pressure (P'), and possibly a uniform end pressure. Thus, the stress components can be written as product time functions. Typically

$$\sigma_{ii}(t) = G_i(t)P_0(t) - F_i(t)P'(t) \qquad (4)$$

(no sum on i)

where the $G_i(t)$ and $F_i(t)$ are geometry functions reflecting the ablating inner radius. Typically, the χ_{11} strain becomes

$$\epsilon_{11} = \int_0^{t_n} D(t_n - t)\left\{G_1\frac{\partial P_0}{\partial t} - F_1\frac{\partial P'}{\partial t} + \frac{\partial G_1}{\partial t}P_0 - \frac{\partial F_1}{\partial t}P' - \frac{1}{2}\left(G_2\frac{\partial P_0}{\partial t} - F_2\frac{\partial P'}{\partial t} + \frac{\partial G_2}{\partial t}P_0 - \frac{\partial F_2}{\partial t}P' + G_3\frac{\partial P_0}{\partial t} - F_3\frac{\partial P'}{\partial t} + \frac{\partial G_3}{\partial t}P_0 - \frac{\partial F_3}{\partial t}P'\right)\right\}dt \qquad (5)$$

No further development along these lines is made. Instead, a completely physical interpretation is given to the problem of the idealized propellant geometry. Equation (5) is helpful in verifying and interpreting the results of the following derivation of useful numerical equations.

Assume that a P_0 history is given (as in Fig. 1) and that the bore-radius history and the uniaxial creep compliance are also given. The P_0 curve is approximated by a series of steps. An ideal geometry, such as a cylinder obeying Lamé's stress relations, is assumed. Real time is used to keep the formulation simple and because isothermal conditions generally prevail during a motor firing.

The Boltzmann principle can be expressed as a finite series of step-stress inputs. θ, r, and z will represent the coordinate directions in the following discussion:

$$\epsilon_\theta(b, t_n) = D(t_n - t_1)\Delta\sigma_1 + D(t_n - t_2)\Delta\sigma_2 + \ldots \qquad (6)$$

Here, we consider ϵ_θ, the propellant hoop strain at the case interface at $t = t_n$, as the quantity that must be made continuous with the case circumferential strain for a typical Lamé cylinder. The analysis also could include a requirement such as compatibility of axial strain between propellant and case, but, here, the object is to formulate the correct step stresses, $\Delta\sigma_j$,† and it is simply stipulated that the cylinder must be compatible with the case at each discrete time point t_j. Between time points, the grain is allowed to creep; compatibility is restored at each time point by applying an increment of interface pressure $\Delta P_j'$. At the same time, P_0 is increased by ΔP_{0j}. These two reactions will cause step changes in the stress components at radius b:

$$\left.\begin{aligned}\Delta\sigma_{\theta j} &= GH_{j-1}\Delta P_{0j} - FH_{j-1}\Delta P_j' \\ \Delta\sigma_{zj} &= GZ_{j-1}\Delta P_{0j} - FZ_{j-1}\Delta P_j' \qquad \Delta\sigma_{rj} = -\Delta P_j'\end{aligned}\right\} \qquad (7)$$

† Subscripts refer to time points.

where the GH, FH, etc., are the geometry constants for the interval in question, e.g., $GH_j = 2a^2/(b^2 - a^2)$ for a Lamé cylinder and $a = a(t_j)$. In addition, the bore radius is assumed to change according to the step approximation of the burning law (similar in principle to Fig. 1) just after each time point is reached. The change in geometry causes an additional set of stress increments:

$$\left.\begin{aligned}\Delta\sigma_{\theta Gj} &= (GH_j - GH_{j-1})P_{0j} - (FH_j - FH_{j-1})P_j' \\ \Delta\sigma_{zGj} &= (GZ_j - GZ_{j-1})P_{0j} - (FZ_j - FZ_{j-1})P_j' \\ \Delta\sigma_{rGj} &= 0\end{aligned}\right\} \qquad (8)$$

With this notation for the stress increments (modifications may be made for spherical shapes), Eq. (6) becomes

$$\epsilon_\theta(b, t_n) = \sum_{j=1}^{j=n} D(t_n - t_{j-1})\left[\Delta\sigma_{\theta j} - \frac{1}{2}(\Delta\sigma_{rj} + \Delta\sigma_{zj})\right] + \sum_{j=1}^{j=n-1} D(t_n - t_j)\left[\Delta\sigma_{\theta Gj} - \frac{1}{2}(\Delta\sigma_{rGj} + \Delta\sigma_{zGj})\right] \qquad (9)$$

Thus, Eq. (9) gives the circumferential strain response at $t = t_n$ to all of the stress increments accruing from $t = 0$. The various pressure and geometry functions and their partial derivatives [Eq. (5)] correspond to the pressure and geometry terms and their finite difference values in Eqs. (7–9). At t_n, it is assumed that all of the quantities are known except the value of $\Delta P_n'$ ($\Delta P_1'$ through $\Delta P_{n-1}'$ being already evaluated), which is found by equating $\epsilon_\theta(b, t_n)$ for the propellant to $\epsilon_{\theta c}$, the case circumferential strain. Thus

$$\sum_{=1}^{n} D(t_n - t_{j-1})\left[\Delta\sigma_{\theta j} - \frac{1}{2}(\Delta\sigma_{rj} + \Delta\sigma_{zj})\right] + \sum_{j=1}^{n-1} D(t_n - t_j)\left[\Delta\sigma_{\theta Gj} - \frac{1}{2}(\Delta\sigma_{rGj} + \Delta\sigma_{zGj})\right] = AP_n' - BP_{0n} \qquad (10)$$

where A and B are combined elastic and geometric constants for the case. Equation (10) can be separated conveniently to yield

$$\Delta P_n'\left\{A + D(t_n - t_{n-1})\left[FH_{n-1} - \frac{1}{2}FZ_{n-1} - \frac{1}{2}\right]\right\} = AP_{n-1}' + BP_{0n} + \sum_{j=1}^{n-1}\left\{D(t_n - t_{j-1})\left[\Delta\sigma_{\theta j} - \frac{1}{2}\times(\Delta\sigma_{rj} + \Delta\sigma_{zj})\right] + D(t_n - t_j)\left[\Delta\sigma_{\theta Gj} - \frac{1}{2}\times(\Delta\sigma_{rGj} + \Delta\sigma_{zGj})\right]\right\} + D(t_n - t_{n-1})\left[GH_{n-1} - \frac{1}{2}GZ_{n-1}\right]\Delta P_{0n} \qquad (11)$$

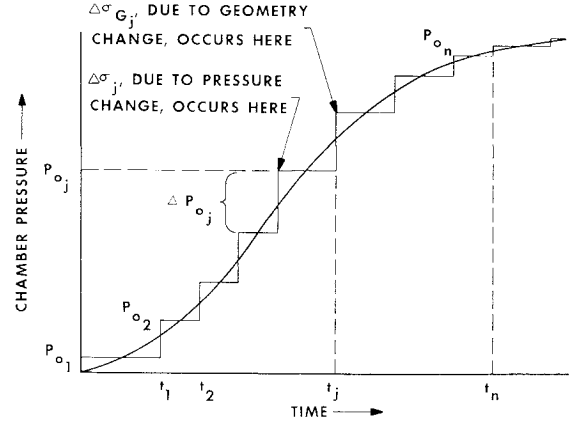

Fig. 1 Step approximation of given pressure-time history.

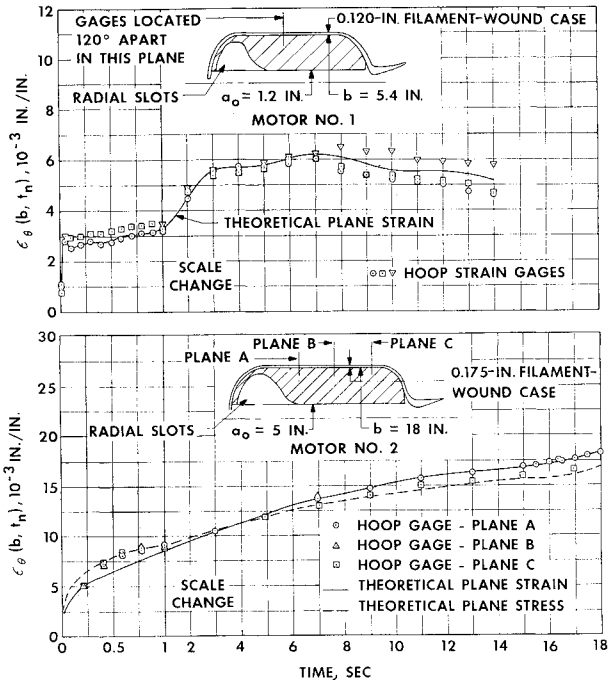

Fig. 2 Theoretical and measured interface strains.

By starting at t_1, all $\Delta P_n'$ are found in order. Equation (11) is programed easily for a digital computer. Of great advantage is the fact that the time increments need not be uniform; thus a rapid ignition rise can be covered adequately without requiring an unwieldy network at later times.

Test Results and Discussion

The influence of the various simplifying assumptions and the usefulness of the method in general are judged best by the comparisons between theory and experiment in Figs. 2–4. The gages measured hoop strains at various locations on the test motors as indicated. The motor cases were filament-wound and therefore relatively flexible, thus giving the grains a good chance to respond. Although the values

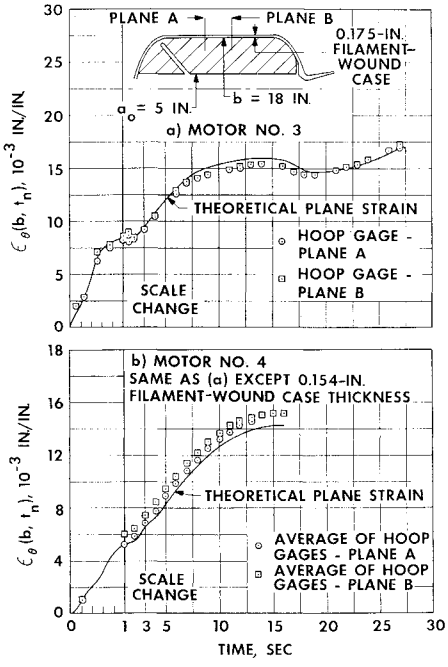

Fig. 3 Theoretical and measured interface strains.

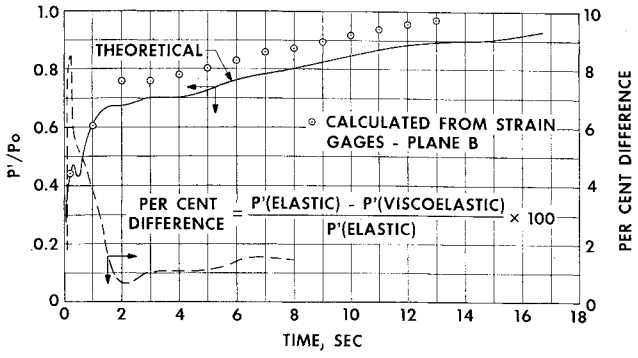

Fig. 4 Interface pressure-to-chamber pressure ratio, a measure of grain response and comparison of interface pressures calculated by viscoelastic and instantaneous elastic methods (motor 4).

of the elastic constants for the cases were rather difficult to calculate exactly, this difficulty is not felt to be serious enough to invalidate the comparison.

An important consequence of this method has been the opportunity to check a simplified elastic solution using the instantaneous value of the creep compliance (or relaxation modulus) and the instantaneous P_0 and geometry. This was done for some of the motors, which were analyzed for comparison with the test data. Except for motor 4 (Fig. 4), there was no significant difference between the stepwise viscoelastic results and the instantaneous elastic results. The two solutions differed noticeably for the last motor, particularly over the short-time region. The last motor had the thinnest case of the series and the propellant with the lowest temperature. Hence, it is concluded that, when the deflection of the grain is controlled chiefly by a relatively rigid motor case, and the time dependent variables do not behave too erratically, the elastic solution is adequate. Fortunately, many practical motor problems will fall into this category, but it may be necessary first to perform a viscoelastic solution.

These results suggest an answer to the original problem of how to calculate the stress-strain field in a finite-length grain. Obviously, if the idealized grain problem is suitable for solutions by the simplified elastic method, then the elastic solution to the finite-length grain also should be satisfactory. If the viscoelastic solution and the instantaneous elastic solution differ for the ideal geometry, it would seem that a reasonable approach would be to use the elastic solution for the finite-length problem, only this time with instantaneous elastic constants, which are back-calculated from the solution for the ideal geometry. It remains, of course, to expand the stepwise approach for direct solution of problems wherein the geometry is other than ideal. In this vein it is felt that the simplified physical interpretation of the superposition integral should be helpful in formulating such problems, as well as other classes of viscoelastic problems, provided that a first boundary-value elastic analogy exists. Aspects of the ablating viscoelastic problem are discussed in detail in the partial list of references.[1–4]

References

[1] Elder, A. S., "Derivation of equations for the stresses and strains in a cylindrical viscoelastic case-bonded grain," Ballistic Research Lab., Aberdeen Proving Ground, Rept. 1359 (1961).

[2] Shinozuka, M., "Stresses in a linear incompressible viscoelastic cylinder with moving inner boundary," American Society of Mechanical Engineers Paper 63-APMW-2 (1963).

[3] Schapery, R. A., "Approximate methods of transform inversion for viscoelastic stress analysis," Proc. U. S. Natl. Congr. Appl. Mech. 4th, 2, 1075–1085 (1962).

[4] Schapery, R. A., "A method of viscoelastic stress analysis using elastic solutions," *Bulletin of the 3rd Meeting of the Working Group on Mechanical Behavior* (Chemical Propulsion Information Agency, The John Hopkins University Applied Physics Laboratory, Silver Springs, Md., 1964), Vol. 1, pp. 27–53.